Dynamic Contrast Enhanced-MRI of the Liver using Automated Navigator Tracker and Prospective Navigator Correction

Takao Goto[1], Shiro Ozaki[2], Yuji Iwadate[3], Kunihiro Miyoshi[1], Koji Uchida[4], Hajime Kitagaki[4], and Hiroyuki Kabasawa[3]

[1]MR Engineering, GE Healthcare, Hino-shi, Tokyo, Japan, [2]Shimane University Hospital, Izumo-shi, Shimane, Japan, [3]Global MR Applications and Workflow, GE Healthcare, Hino-shi, Tokyo, Japan, [4]Department of Radiology, Shimane University Faculty of Medicine, Izumo-shi, Shimane, Japan

PURPOSE: In our previous study, we proposed a method of automated placement of a navigator tracker[1] (ANAV) to improve operator workflow and achieve a consistent examination independently of the skills possessed by an operator. Although we demonstrated that the positioning of the ANAV was robust for a variety of images, the evaluation of a navigator echo sequence using ANAV is yet to be pursued. The goal of this research is to apply the ANAV technique to dynamic contrast-enhanced (DCE) liver-MRI and evaluate the performance of prospective navigator echo correction.

METHOD: Usual 2D scout images are analyzed by the ANAV algorithm, which first extracts the 2D shape of the dome of the right hemi-diaphragm via an ensemble machine learning technique[2]. It then places a navigator tracker automatically on the peak of the dome in the right/left (R/L) and the superior/inferior (S/I) direction of the coronal image (Fig.1a). This navigator tracker is also at the middle of the thorax height in the anterior/posterior (A/P) direction of the axial image[3] (Fig.1b). DCE liver-MRI uses breath-holding scans to avoid motion effects. However, different depths of breath-holds of a subject changes the position of the liver in every dynamic phase. As this is dependent on an individual, the different liver positions are imaged in each phase even if the excited slice location is identical. Therefore, a prospective navigator echo sequence is often used to compensate for the shift[4]. It detects the dome position in the S/I direction (Fig. 2a) and prospectively changes the slice location of the successive imaging sequence to obtain the same liver position in the image (Fig. 2b), if the detected dome position is different from the reference position. This difference can be computed by cross correlation of the referenced and current 1D Fourier-transformed navigator echo signals before commencing the imaging sequence. Consequently, the same locations of the liver are imaged through every phase even if the depth of the breath-hold of a subject varies among each dynamic phase. In our evaluation, a T1 weighted fat-saturated 3D fast SPGR sequence is used for the DCE MRI, whose scan parameters were given as TR/TE: 3.5/1.7 ms; scan matrix: 320 × 192; slice thickness: 2.5 mm; number of slices after slice interpolation: 76 axial slices; NEX: 0.71; and FOV: 340 × 340 mm. The total scan time was approximately 15 s using a higher parallel imaging acceleration factor. Other than DCE MRI, dual echo 3D fast gradient echo was used as the reference to the pre-contrast image, whose parameters were TR/TE1/TE2: 5.6/1.3/2.7 and the others being the same as DCE MRI. The navigator echo sequence was designed based on a gradient echo sequence. To prevent a saturation band in images owing to an excitation pulse of the navigator, a "pencil-beam" 2D radio frequency excitation pulse[5], with a width of 10 – 20 mm and a length of approximately 100 mm, excites the region. We set the dome position of the pre-contrast image as the reference. The successive navigator echoes in the sequences of arterial, portal, equilibrium, and two delayed phases were then used to detect the dome positions and track the dome position of the reference. To evaluate the effect of the navigator, we measured how many slices had to be shifted to observe the same liver image between the reference and objective images. This measurement was pursued by one MR application specialist and one scientist in the field of image processing. The first five slices from the top of the liver dome were used for the measurement. Furthermore, the five slices in the middle and the other five slices from the bottom were also measured. For the case without the navigator, we anticipated the amount of the slice shift by dividing the computed value (Δd in Fig. 2) by the thickness of a slice. We tested 40 patients (mean age = 64 years; age range = 24 – 85 years) after informed consent was obtained from every volunteer under institutional review and approval.

RESULTS: The navigator tracker was placed automatically for each patient only once by the error of 6.3 mm standard deviation for the target position. Fig. 3 shows the distribution of the slice shift (a) with and (b) without the navigator for the top five slices. The standard deviations of with and without the navigator were the shifts of 2.04 and 5.33 slices respectively. The maximum was a shift of 4 slices even with the application of the navigator. Table 1 lists the percentages within a shift of one or two slices except for the case where the liver was deformed. The top and bottom portions of the liver were well tracked by more than 95%. There were no cases that worsened the slice shift by applying the navigator.

DISCUSSION: The navigator sequence worked correctly by the ANAV method. A few cases still presented a shift of 3–4 slices, which was caused by the deformation of the liver due to a significant difference in the depth of the breath. Further, a patient may move due to impatience leading to further error. Fig. 4 shows the reformatted coronal images of the pre-contrast and arterial phases when the slice shift was still three even with navigator tracking utilized. In our observation, a shift greater than four slices (1 cm) makes it more difficult to compensate perfectly since the motion is not represented by a rigid translation. Currently, this poses a limitation of the current navigator method.

Conclusion: We have demonstrated that the prospective navigator correction with the ANAV method was effective for the DCE liver-MRI method on a group of 40 patients. Our practical approach is expected to assist operator tasks through the navigator sequence.

References

[1]. Goto T. et al. ISMRM2014 1614
[2]. Freund Y, Schapire RE. et al. Compute. Syst. Sci. 1997;61:19–139
[3]. Goto T. Ito S. MICCAI Workshop ABDI2014 LNCS8676 (in press)
[4]. McConnel MV. et al. MRM 1997;37:148-152
[5]. Nehrke K. et al. MRI 1999;17:1173-1181

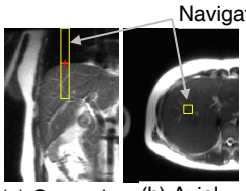

Fig. 1 Auto navigator Tracker placement

Table 1. Total shift of slices by a navigator.

	Top	Mid	Bottom
Within 1 slice shift	95.4	92.7	95.9
Within 2 slices shift	98.2	93.6	95.9
More than 2 slices	1.83	2.29	1.83

Unit [%]

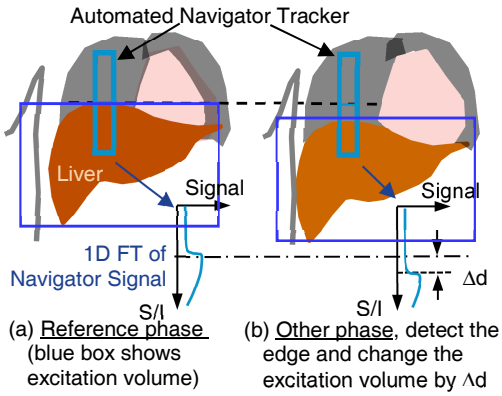

Fig. 2 Slice tracking by navigator echo

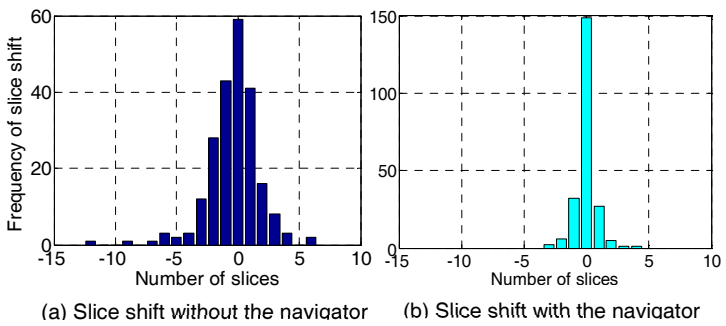

Fig. 3 Distribution of slice shift

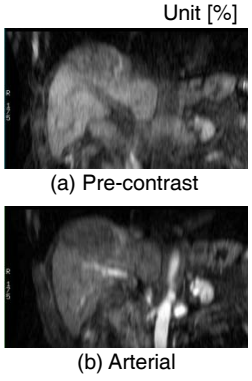

Fig. 4 Reformatted images